

# Breakdown of Migdal–Eliashberg theory via catastrophic vertex divergence at low phonon frequency

J.P.Hague

*Department of Physics, University of Warwick, CV4 7AL, U.K. and  
Department of Physics, Loughborough University, LE11 3TU, U.K.\**

N.d'Ambrumenil

*Department of Physics, University of Warwick, CV4 7AL, U.K.*

(Dated: 25/09/2007)

We investigate the applicability of Migdal–Eliashberg (ME) theory by revisiting Migdal's analysis within the dynamical mean-field theory framework. First, we compute spectral functions, the quasi-particle weight, the self energy, renormalised phonon frequency and resistivity curves of the half-filled Holstein model. We demonstrate how ME theory has a phase-transition-like instability at intermediate coupling, and how the Engelsberg–Schrieffer (ES) picture is complicated by low-energy excitations from higher order diagrams (demonstrating that ES theory is a very weak coupling approach). Through consideration of the lowest-order vertex correction, we analyse the applicability of ME theory close to this transition. We find a breakdown of the theory in the intermediate coupling adiabatic limit due to a divergence in the vertex function. The region of applicability is mapped out, and it is found that ME theory is only reliable in the weak coupling adiabatic limit, raising questions about the accuracy of recent analyses of cuprate superconductors which do not include vertex corrections.

PACS numbers: 71.10.Fd, 71.30.+h, 71.38.Ht, 71.38.Mx

Keywords: Interacting electron systems, electron-phonon interactions, migdal-eliasberg theory

## I. INTRODUCTION

The use of Migdal–Eliashberg (ME) theory for the study and analysis of electron-phonon systems is widespread. For conventional superconductors such as lead, where the electron-phonon coupling is higher than can be treated with BCS theory, ME theory has been extremely successful for understanding the superconducting properties. Recently, a lot of researchers have been interested in an apparent kink in the electronic dispersion of cuprate superconductors as determined from angle

---

\*Electronic address: J.P.Hague@lboro.ac.uk

resolved photo-emission spectroscopy (ARPES), and their analysis / interpretation typically uses the related Engelsberg–Schrieffer (ES) result (i.e. just the lowest order Fock diagram) [1, 2, 3]. The ES result divides excitations into long-lived (coherent) low-energy excitations, and rapidly decaying high-energy excitations, with a kink at the phonon energy. ES based analysis of ARPES results suggests a large electron-phonon coupling in the cuprates, with estimates of the dimensionless coupling constant lying between  $\sim 0.3$  and  $1.5$  (depending on doping) and very large phonon frequencies of  $\sim 50$  meV [3]. There has also been a development of a maximum entropy technique for analysing cuprate superconductors which makes use of Eliashberg theory [4]. The analysis in Ref. 4 determines a dimensionless electron-phonon coupling of  $\lambda > 1$ , but this is well above the  $\lambda \sim 1$  value where one would normally expect perturbation theory to fail. The region of intermediate electron-phonon coupling is also relevant to a number of other materials. For example, electron paramagnetic resonance measurements on the manganites support a strong “electron-phonon” coupling leading to Jahn–Teller polarons [5]. In light of the current experimental situation, and the importance of the conclusions of Refs. 2, 4, a full re-analysis of the perturbation theory is of high significance.

The neglect of vertex corrections suggested by Migdal leads to a theory where an infinite set of Feynman diagrams may be summed. According to an analysis carried out by Migdal, this theory should be valid in the physical regime of electron-phonon problems, where the phonon energy is significantly smaller than the intersite hopping (“Migdal’s theorem”) [6, 7] specifically that the vertex corrections are small when  $\lambda\omega_0/\epsilon_f \ll 1$  ( $\omega_0$  is the phonon frequency and  $\epsilon_f$  the Fermi energy) [34]. On the basis of Migdal’s analysis, it is often believed that Migdal–Eliashberg theory is applicable above  $\lambda \sim 1$  in the adiabatic limit because of the apparently small size of the vertex corrections, even though in general perturbative approaches break down (i.e. the functional form of the self-energy becomes incorrect) when the coupling constant becomes large. In this article, we revisit Migdal’s analysis by examining the large- $d$  limit (local approximation).

The large- $d$  limit has been an effective workshop for determining the validity of approximate schemes. The quantum Monte-Carlo (QMC) solution in the large- $d$  limit [8, 9] has been compared with a number of different diagrammatic approaches [10, 11, 12] demonstrating that self-consistent second-order perturbation theory worked better than Migdal–Eliashberg theory at intermediate phonon frequencies and strong coupling ( $\omega_0 \sim 0.2t$ ,  $U > t$ ). The QMC solution is difficult for very low phonon frequency and low temperature. QMC self-energies and Green functions are generated along the Matsubara axis. As such, it is not easy to make quantitative conclusions about the point of breakdown of ME theory as small differences at individual Matsubara frequencies may result in

relatively large differences in the spectral functions. Using an alternative approach, Benedetti *et al.* [13] found the formation of more than one extremum in the path-integral formulation at very low phonon frequencies and intermediate coupling, leading to a breakdown of ME theory. Work on the finite-dimensional Holstein model also shows deficiencies in ME theory. On the basis of a comparison with exact diagonalization results, Alexandrov *et al.* [14] have shown that ME theory may break down at intermediate couplings even in the adiabatic limit.

In this article, we investigate the Holstein model of electron-phonon interactions [15], which employs a number of approximations. The phonon dispersion is flat corresponding to independently moving ions and phonon anharmonicity is neglected, resulting in a Hamiltonian,

$$H = -t \sum_{\langle ij \rangle \sigma} c_{i\sigma}^\dagger c_{j\sigma} + \sum_{i\sigma} (gx_i - \mu) n_{i\sigma} + \frac{M\omega_0^2}{2} \sum_i x_i^2 + \frac{1}{2M} \sum_i p_i^2, \quad (1)$$

where  $c_{i\sigma}^\dagger$  ( $c_{i\sigma}$ ) create (annihilate) electrons at site  $i$  with spin  $\sigma$ ,  $x_i$  is the local ion displacement,  $p_i$  the ion momentum,  $M$  the ion mass,  $t$  the electron hopping parameter and  $\mu$  the chemical potential. A mean-field Coulomb pseudopotential may also be included, but in the normal state, it is just absorbed into the chemical potential. In the following,  $t = 0.5$  and all energies (including temperature) are measured in units of  $2t$ .

An expression for the effective interaction between electrons can be obtained by performing a linear transformation in the phonon variable to remove the electron-phonon term [16]. The resulting interaction is retarded, with Fourier components:

$$U(i\omega_s) = - \left( \frac{g^2}{M\omega_0^2} \right) \frac{\omega_0^2}{(\omega_s^2 + \omega_0^2)} = -U \frac{\omega_0^2}{(\omega_s^2 + \omega_0^2)}, \quad (2)$$

where  $\omega_s = 2\pi sT$  are the Matsubara frequencies for Bosons. Taking the limit  $\omega_0 \rightarrow \infty$ ,  $g \rightarrow \infty$ , while keeping the ratio  $g/\omega_0$  finite, leads to an attractive Hubbard model [17] with instantaneous attraction of magnitude  $U = g^2/M\omega_0^2 \equiv W\lambda$ , where  $W$  is the half band-width (note that  $U$  is related to the bipolaron binding energy for the strong coupling two-electron problem). In the opposite limit ( $\omega_0 \rightarrow 0$ ,  $M \rightarrow \infty$ , keeping  $M\omega_0^2 \equiv \kappa$  finite) the phonon kinetic-energy vanishes, leaving only a static variable  $x_i$  representing the phonon subsystem in the Hamiltonian,  $H = -t \sum_{\langle ij \rangle \sigma} c_{i\sigma}^\dagger c_{j\sigma} + \sum_{i\sigma} (gx_i - \mu) n_{i\sigma} + \frac{\kappa}{2} \sum_i x_i^2$ . Thus the problem looks like that of a single electron in a disordered potential. The large- $d$  limit of this model was exactly solved by Millis *et al.* [18] and extended to deal with long range order by Ciuchi *et al* [19]. Thus, the phonon frequency may be thought of as a parameter for tuning the level of electronic correlation [20].

In this paper, we investigate the validity of the Migdal–Eliashberg approach within the dynamical mean-field theory formalism. As we carry out the self-consistency on the real-axis self-energies,

we can investigate the behaviour of ME theory over a full range of temperatures and phonon frequencies. We begin by calculating self-energies, spectral functions, the quasi-particle weight and renormalized phonon frequency. To determine the validity of the theory, we calculate an expression for the lowest-order correction to the vertex function, and evaluate its magnitude. We find that the theory can also break down in the low frequency regime, contrary to the standard interpretation of Migdal's analysis. Finally, we calculate resistivity curves in the regime where the lowest-order corrections are small.

## II. MIGDAL-ELIASHBERG THEORY IN THE LOCAL APPROXIMATION

In this article, we use the local approximation or dynamical mean-field theory (DMFT) as a way of analysing the Migdal-Eliashberg theory. The self-energy of correlated-electron systems is momentum independent in limit of large dimensions [21], and approximately momentum independent in 3D. In large- $d$ , lattice models map onto Anderson impurity models with a self-consistent hybridisation [22].

The self-consistent DMFT equations may be obtained by rewriting the action for the model to be considered in terms of an effective single-site action [23]

$$S_{\text{eff}} = - \int_0^\beta d\tau \int_0^\beta d\tau' \sum_\sigma c_{i\sigma}^\dagger(\tau) \mathcal{G}_0^{-1}(\tau - \tau') c_{i\sigma}(\tau') + S_{\text{int}}. \quad (3)$$

Here  $\mathcal{G}_0(i\omega_n)$  plays the rôle of the host Green function in the equivalent impurity model. If one assumes that correlations carried via the bath between electrons entering and exiting a single site can be neglected (true in the case of large coordination number), the degrees of freedom associated with all but one site can be integrated out. This leads to the following self-consistent equation [23],

$$\mathcal{G}_0^{-1}(i\omega_n) = i\omega_n + \mu + G^{-1}(i\omega_n) - R[G(i\omega_n)], \quad (4)$$

where  $G(i\omega_n)$  is the site-local (impurity) Green function, and is itself a functional of  $\mathcal{G}_0(i\omega_n)$ .  $\omega_n = 2\pi T(n + 1/2)$  are the Fermionic Matsubara frequencies.  $R[x]$  is the reciprocal function of the Hilbert transform, defined as  $R[\tilde{D}(\xi)] = \xi$ . The Hilbert transform of the non-interacting density of states,  $\mathcal{D}(\varepsilon)$ , is defined as  $\tilde{D}(\xi) \equiv \int_{-\infty}^{+\infty} d\varepsilon \mathcal{D}(\varepsilon)/(\xi - \varepsilon)$ .

When electrons move on a tight-binding hypercubic lattice, the bare DOS takes the form of a Gaussian [21],  $\mathcal{D}(\varepsilon) = \exp(-\varepsilon^2/2t^2)/t\sqrt{2\pi}$  and there is no simple expression for the reciprocal function. Introducing the modified Dyson equation,

$$\mathcal{G}_0^{-1}(i\omega_n) = G^{-1}(i\omega_n) + \Sigma(i\omega_n), \quad (5)$$

(where  $\Sigma(i\omega_n)$  is the electron self-energy), equation (4) may be rewritten as,

$$R[G(i\omega_n)] = i\omega_n + \mu - \Sigma(i\omega_n), \quad (6)$$

and inverted to give an expression for the Green function in terms of the self-energy,

$$G(i\omega_n) = \int \frac{d\varepsilon \mathcal{D}(\varepsilon)}{i\omega_n + \mu - \Sigma(i\omega_n) - \varepsilon}. \quad (7)$$

This also allows the approximation to be interpreted as a coarse graining of the momentum space [24]. To complete the scheme, a form for the electronic self-energy must be calculated in terms of the non-interacting Weiss field. This is normally approximate. Then a self-consistent procedure is followed: Compute the Green function from equation (7), the Weiss field from equation (5) and then re-calculate the self-energy until convergence is reached.

The application of ME theory within DMFT corresponds to computing the self-energy and phonon propagator from the diagrammatic equations in figure 1(a and b). The self-consistent solution of such a self-energy corresponds to the summation of all Feynman diagrams which contain no vertex corrections. In the low (non-zero) phonon-frequency limit, Migdal's analysis indicates a condition,  $U\omega_0 \ll t^2$ , for the neglect of corrections to the vertex function [6].

The solution of the Dyson equation seen in figure 1(a) results in the full phonon propagator,

$$D(\omega) = \frac{\omega_0^2}{(\omega + i\eta)^2 - \omega_0^2[1 + \Pi_0(\omega)]}, \quad (8)$$

which is then used for the calculation of the electron self-energy. The phonon polarisation bubble (dimensionless self-energy)  $\Pi_0(i\omega_s)$  is given from perturbation theory,

$$\Pi_0(i\omega_s) = -2UT \sum_m G(i\omega_m)G(i\omega_s + i\omega_m), \quad (9)$$

and may be analytically continued by introducing the spectral representation,  $G(i\omega_n) = \int dx \rho(x)/(i\omega_n - x)$  where  $\rho(\omega) = \text{Im}[G(\omega + i\eta)]/\pi$  and performing the sum over Matsubara frequencies to give,

$$\text{Im}[\Pi_0(\omega)] = -2U \int_0^\omega dx \rho(-x)\rho(\omega - x), \quad (10)$$

at absolute zero, and

$$\text{Im}[\Pi_0(\omega, T)] = -U \sinh\left(\frac{\omega}{2T}\right) \int_{-\infty}^{\infty} dx \frac{\rho(-x)}{\cosh\left(\frac{x}{2T}\right)} \frac{\rho(\omega - x)}{\cosh\left(\frac{\omega - x}{2T}\right)}, \quad (11)$$

at finite  $T$ . The full spectral function is used so that all diagrams with no vertex corrections are included, consistent with the proper interpretation of Migdal's analysis.

The lowest-order skeleton diagram shown in figure 1(b),

$$\Sigma(i\omega_n) = -UT \sum_s G(i\omega_n - i\omega_s) D(i\omega_s), \quad (12)$$

may be analytically continued in the same way as the polarisation bubble to give,

$$\text{Im}[\Sigma(\omega)] = U \int_0^\omega dx \rho(x) \sigma(\omega - x), \quad (13)$$

with  $\sigma(\omega) = \text{Im}[D(\omega + i\eta)]/\pi$ . A more complicated expression applies at finite temperature,

$$\text{Im}[\Sigma(\omega)] = U \cosh\left(\frac{\omega}{2T}\right) \int_{-\infty}^{\infty} \frac{dx \rho(\omega - x) \sigma(x)}{2 \cosh\left(\frac{\omega-x}{2T}\right) \sinh\left(\frac{x}{2T}\right)}. \quad (14)$$

At each stage, the Kramers–Kronig relation is used to compute the real parts of the electron and phonon self-energies, for instance  $\text{Re}[\Pi_0(\omega)] = \text{P} \int dx \text{Im}[\Pi_0(x)]/\pi(\omega - x)$ , where P denotes the principal integral.

After the self-consistent procedure has converged, physical properties are calculated, including the quasi-particle weight (inverse effective mass),

$$Z = \frac{m_0}{m^*} = 1 - \left. \frac{\partial \Sigma}{\partial \omega} \right|_{\omega=0}, \quad (15)$$

the effective phonon frequency  $\Omega$  from,

$$\Omega^2 - \omega_0^2(1 + \text{Re}[\Pi_0(\Omega)]) = 0, \quad (16)$$

and the optical conductivity [25],

$$\text{Re}[\sigma(\omega)] = \frac{\pi}{\omega} \int_{-\infty}^{\infty} d\varepsilon \mathcal{D}(\varepsilon) \int_{-\infty}^{\infty} d\nu \rho(\varepsilon, \nu) \rho(\varepsilon, \nu + \omega) [f(\nu) - f(\nu + \omega)], \quad (17)$$

where  $f(x)$  is the Fermi-Dirac distribution and  $\rho(\varepsilon, \nu) = \text{Im}[1/(\nu + i\eta - \varepsilon - \Sigma(\nu))]/\pi$  (taking the limit,  $\omega \rightarrow d\omega$ , the DC conductivity is recovered.)

Although DMFT is approximate, the formalism can be expected to work in the non-interacting limit, where coarse graining will give the exact non-interacting DOS for the tight-binding model (regardless of dimension). In the opposite limit ( $t \rightarrow 0$ ), the neglect of loops through the host is justified, and the formalism should be exact. Such propagation of correlation is also small when the coordination number is high (e.g. FCC lattices).

### III. SPECTRAL PROPERTIES

We have solved the DMFT equations using the self-energies in equations (13) and (14) to find electron spectral functions. We show the evolution of these functions with coupling for  $\omega_0 = 0.125$

in figure 2(a) and  $\omega_0 = 0.5$  in figure 2(b). The spectral functions show two features. There is a low energy peak with a width defined by the phonon frequency, and a high energy shoulder. This behaviour can be related to the two limits of the Holstein model. At low energy scales ( $\omega < \omega_0$ ), electrons interact via virtual processes and the behaviour is essentially Hubbard-like (correlated). At frequencies greater than  $\omega_0$ , the spectral weight is reduced, phonons may be created, and static behaviour emerges (in the static limit, phonons may always be created as no energy is required to deform the lattice). The central peak narrows with increased coupling, until a critical value is reached. Here, the theory has a Brinkman–Rice-like transition with a diverging effective mass [26].

In figure 3, we plot the imaginary part of the self-energy. For low coupling strengths (small  $U$  and energy scales ( $|\omega| < \omega_0$ ),  $\text{Im}[\Sigma(\omega)]$  is small because electrons cannot create phonons, consistent with the Englesberg–Schrieffer analysis). However, as the coupling increases, electrons can be scattered by bipolaron resonances and  $\text{Im}[\Sigma(\omega)]$  rises sharply on either side of the Fermi-energy. The gap in the weight of the self-energy is frequently assumed in the analysis of ARPES data, but as we can see here, when the electron-phonon coupling approaches the band width (i.e.  $\lambda \sim 1$ ), the self-energy has a more complicated form, without the simple picture of coherent and incoherent quasi-particles. Indeed, it has been demonstrated that in low dimensions, vertex corrections are required to achieve a sharp discrimination between coherent and incoherent dressed electrons [27].

The onset of this “transition” can be studied by examining the inverse quasi-particle mass (quasi-particle weight), shown in figure 4 for two values of phonon frequency. As the coupling increases,  $Z$  becomes smaller and eventually vanishes at a critical value of coupling (the effective mass diverges).

We also examine the phonon spectral function in figure 5 for  $\omega_0 = 0.125$  and various couplings. As the coupling is increased, the phonon modes soften (figure 6). The effective frequency does not tend to zero as quickly as the quasi-particle weight. We will revisit this point later in this article.

It is clearly the case that ME theory does not correctly describe the strong coupling limit. It is known from the exact solution of the static limit [18] and from approximate “iterated-perturbation theory” [28] and QMC [29] solutions of the Hubbard model, that sub-bands should form at strong coupling. As our calculations demonstrate, this sub-band formation is not properly reproduced within ME theory and this makes it likely that effects of vertex corrections become significantly more important at strong coupling. Since this is at variance with the traditional interpretation of Migdal’s analysis, we are motivated to re-examine the vertex function in the next section.

#### IV. BREAKDOWN OF MIGDAL–ELIASHBERG THEORY

The neglect of the lowest-order vertex correction shown in figure 1(c) and all higher-order corrections is central to Migdal–Eliashberg theory. In this section, we compute the lowest-order correction and use this to define the region of validity for ME theory. In this sense, we are revisiting Migdal’s analysis to understand why there is a contradiction between low frequency results computed with ME theory and advanced numerical methods.

The ratio of first to zeroth order vertices at finite temperature may be written as

$$\frac{\Gamma_1(i\omega_n, i\omega_x)}{\Gamma_0} = TU \sum_s \mathcal{G}_0(i\omega_n - i\omega_s) \mathcal{G}_0(i\omega_n - i\omega_s - i\omega_x) D_0(i\omega_s). \quad (18)$$

As temperature tends to zero, this sum becomes an integral which may easily be evaluated ( $x$  and  $\omega$  are defined as in figure 1),

$$\frac{\Gamma_1(i\omega, ix)}{\Gamma_0} = \frac{U}{2\pi} \int ds \mathcal{G}_0(i\omega - is) \mathcal{G}_0(i\omega - ix - is) D_0(is). \quad (19)$$

In order for vertex corrections to be unimportant, the ratio  $\Gamma_1/\Gamma_0$  must be small. As an example, we show the lowest order correction to the vertex function for (a)  $\omega_0 = 0.0556$  and  $U = 0.214$  (b)  $\omega_0 = 0.75$  and  $U = 0.214$  in figure 7. For the larger phonon frequencies, the ratio is clearly greater than 10% and the approximation is expected to be significantly changed by the inclusion of vertex corrections. For the weak coupling  $U$  shown here, the corrections are much less pronounced for small phonon frequencies.

In Figure 8 we show the magnitude of the central peak of the vertex correction (always the largest part of the function) for a range of couplings at  $\omega_0 = 0.0556$ . Between  $U = 0.54$  and  $U = 0.55$  the vertex correction diverges, and ME theory clearly breaks down. As it is necessary to pass through the divergence to reach  $U > 0.545$ , the theory is not applicable for strong couplings.

Figure 9 shows the lowest value of  $U' = U/(t + U)$  for given  $\omega'_0 = \omega_0/(t + \omega_0)$  at which the ratio  $\Gamma_1/\Gamma_0$  exceeds 0.1 (the primed quantities are chosen so that  $U' = 1$  represents an unprimed value  $U = \infty$ , and a primed value of  $U' = 0.5$  represents an unprimed value  $U = t$ ). Below this value ME theory can be expected to give accurate results, while the theory begins to break down above this line. For  $\omega'_0 \gtrsim 0.2$  ( $\omega_0 \gtrsim 0.125$ ) the standard Migdal criterion works well and correctly predicts the region in which ME theory is applicable. However for frequencies  $\omega'_0 \lesssim 0.2$  ( $\omega_0 \lesssim 0.125$ ), the Migdal criterion misses the divergence in the vertex correction associated with the divergence in the effective mass. This breakdown happens at  $U \sim t$  or  $\lambda \sim 1$ . The line of breakdown due to this vertex divergence levels off as the phonon frequency approaches zero and does not scale as  $1/U$



(Migdal's criterion). These results imply that there is a breakdown in ME theory in the adiabatic limit.

We note that at high phonon frequencies ( $U, t \ll \omega_0$ ), our line does not tend to zero. This is because the contribution  $\Gamma_1/\Gamma_0(x \rightarrow 0, \omega' \rightarrow 0)$  does not tend to infinity. Instead, the function gets wider as the phonon frequency increases (see figure 7, panel b), and some combination of the magnitude and width of the vertex is probably a better measure of the importance of vertex corrections. At large  $\omega_0$ , the breakdown is quite different to that at low phonon frequencies as the second order diagrams (one of which contains a vertex correction) develop the same functional form and magnitude. However the breakdown at  $U = 0.1$  ( $U' = 0.17$ ) is not too bad an estimate. At this value of  $U$ , there is only a small mass renormalisation due to vertex corrections.

Our results are consistent with that of Benedetti and Zeyher [13], which was obtained with a different technique using a semi-circular density of states ( $\mathcal{D}_{SC}(\epsilon) = \sqrt{4t^2 - \epsilon^2}/2\pi t^2$ ), and predicted breakdown for  $\lambda_{SC} \geq 1.25$  in the extreme adiabatic limit. We have included their result in the figure, choosing the bandwidth parameter by matching the bare DOS at the Fermi energy for the two cases (the conversion factor is  $\lambda = \mathcal{D}_{SC}(0)\lambda_{SC}/\mathcal{D}(0) = \lambda_{SC}\sqrt{2/\pi}$ ) which is reasonable when considering low energy excitations at half-filling, and corresponds to a critical  $\lambda \geq 0.997$  for the Gaussian DOS used here (see the diamond in figure 9). Millis *et al.* [18] also predicted a breakdown in ME theory at  $U \sim t$  from their solution of the static limit of the infinite-dimensional Holstein model, consistent with the breakdown that we have found. The solution of the static limit predicts the formation of sub-bands, which is something not reproduced in the ME solution. The lack of subbands in ME theory demonstrates that higher order diagrams are essential for the description of the sub-band formation, and therefore for the description of the strong coupling limit.

We suggest that the breakdown of ME theory should be understood in the following heuristic manner. As the coupling increases, the host spectral function ( $\mathcal{G}_0$ ) narrows and spectral weight is shifted towards lower energy scales. There is then an effective bandwidth,  $t_{\text{eff}} < t$ , for quasi-particles close to the Fermi surface. The condition for the applicability of ME theory then becomes  $U\Omega \ll t_{\text{eff}}^2 \sim Z^2$ . As seen in figure 5, there is also a reduction in the effective phonon frequency with increasing interaction strength. Although the renormalisation of the phonon frequency helps to drive against the transition, we note that the band narrowing effect is much stronger, as can be seen by comparing figures 4 and 6.

## V. RESISTIVITY CURVES

Using the finite temperature form of the self-energy, it is possible to calculate resistivity curves. These are shown in figure 10 at various electron-phonon coupling and phonon frequency. At high temperatures, the tendency is to linear behavior, with a gradient depending on  $U$ , but independent of  $\omega_0$ . The effect of phonon frequency is most dramatically seen at  $T \sim \omega_0/2$ , where a point of inflection is seen, before the curve tends to low temperature  $T^2$  behavior, consistent with a weakly renormalized electron gas. We note that long range order has not been considered in this study, so no superconducting transition is seen. The negative curvature of the resistivity curve at intermediate temperatures is of interest, since that curvature has recently been interpreted as an onset of the Mott limit, but may have a different interpretation as an intermediate coupling phenomenon [30].

## VI. CONCLUSIONS

We have computed spectral functions, resistivity curves, self-energies, quasi-particle weight and effective phonon frequency for the Holstein model at half-filling using Migdal–Eliashberg theory, within the DMFT framework, and revisited Migdal’s analysis of the strength of the vertex correction. By analysing the first order vertex correction, we have defined the region of applicability of ME theory. We find that ME theory breaks down at intermediate coupling in the adiabatic limit, showing that Migdal–Eliashberg theory should only be trusted at weak coupling within this framework. The coupling at which breakdown occurs corresponds to a divergence in the effective mass, indicating that both long range order and vertex corrections should be included to correctly describe the strong coupling regime.

The question remains: What was lacking from the analysis of Migdal, which estimated the magnitude of the vertex corrections. This can be understood from the magnitude of the kinetic energy. In the calculations, the kinetic energy can be seen to be decreasing due to the localisation at the non-analyticities. Thus in Migdal’s estimate, the renormalised kinetic energy, and not the bare kinetic energy should have featured. The renormalised phonon frequency should also have been used, but it tends to zero more slowly than the kinetic energy. At the non-analyticity, where the kinetic energy tends to zero, it can be seen that a vertex divergence is expected from the modified version of Migdal’s estimate.

Our results are timely because of a recent upsurge of interest in the role of electron-phonon

coupling in the cuprate superconductors. There are many experimental results which have been analysed and interpreted using ES/ME theory, in spite of the large coupling constant that has been predicted from that analysis. Many groups are using Migdal's analysis to justify their claims, without a careful consideration of the self-consistent effect of coupling on the kinetic energy of the electrons (polarons). Exact numerical analysis shows that large electron-phonon couplings significantly reduce the kinetic energy of electrons [31] and thus affect the internal consistency of Migdal's analysis. Therefore, the any very large  $\lambda$  determined from ES style analysis of experimental results is not consistent with a theory that neglects vertex corrections (i.e. a more detailed analysis with higher order effects included is necessary). Without that analysis, the only conclusion that can be reached is that the coupling is large, but no reliable value for that coupling can be determined. The main conclusion of a breakdown is not expected to change in 1D, 2D or 3D. In three dimensional systems, the role of spatial fluctuations should only be significant very close to the bi-polaron instability. The role of spatial fluctuations on the spectral properties in 2D has been analysed at weak coupling, and is found to lead to quantitative differences in the coherent excitations [27]. Spatial fluctuations have a major role in the superconducting state, and it has also been shown that the Eliashberg approach to superconductivity is inadequate for optical phonon mediated *d*-wave superconductivity [32], and incomplete for *s*-wave superconductivity [33]. We therefore urge researchers to carefully analyse the internal consistency of their theories when dealing with strong coupling materials.

## VII. ACKNOWLEDGEMENTS

The authors would like to thank F.Gebhard and F.Essler for useful discussions. JPH thanks the EPSRC for partial funding of this work.

- 
- [1] S. Engelsberg and J. R. Schrieffer, Phys. Rev. **131**, 993 (1963).
  - [2] T. Cuk, F. Baumberger, D. H. Lu, N. Ingle, X. J. Zhou, H. Eisaki, N. Kaneko, Z. Hussain, T. P. Devereaux, N. Nagaosa, Z. -X. Shen, Phys. Rev. Lett. **93**, 117003 (2004).
  - [3] A. Lanzara, P. V. Bogdanov, X. J. Zhou, S. A. Kellar, D. L. Feng, E. D. Lu, T. Yoshida, H. Eisaki, A. Fujimori, K. Kishio, J. -I. Shimoyama, T. Noda, S. Uchida, Z. Husa, Z. -X. Shen, Nature **412**, 6846 (2001).
  - [4] J. Hwang, T. Timusk, E. Schachinger, and J. P. Carbotte, Phys. Rev. B **75**, 144508 (2007).
  - [5] G. M. Zhao, K. Conder, H. Keller, and K. A. Müller, Nature **381**, 676 (1996).

- [6] A. B. Migdal, Soviet Physics JETP **7**, 996 (1958).
- [7] G. M. Eliashberg, Soviet Physics JETP **11**, 696 (1960).
- [8] J. K. Freericks, M. Jarrell, and D. J. Scalapino, EuroPhysics Letters **25**, 37 (1994).
- [9] J. Hirsch and E. Fradkin, Phys. Rev. B **27**, 4302 (1983).
- [10] J. K. Freericks and M. Jarrell, Phys. Rev. B **50**, 6939 (1994).
- [11] J. K. Freericks, V. Zlatić, W. Chung, and M. Jarrell, Phys. Rev. B **58**, 11613 (1998).
- [12] J. K. Freericks, M. Jarrell, and D. J. Scalapino, Phys. Rev. B **48**, 6302 (1993).
- [13] P. Benedetti and R. Zeyher, Phys. Rev. B **58**, 14320 (1998).
- [14] A. S. Alexandrov, V. V. Kabanov, and D. K. Ray, Phys. Rev. B **49**, 9915 (1994).
- [15] T. Holstein, Ann. Phys. **8**, 325 (1959).
- [16] N. E. Bickers and D. J. Scalapino, Ann. Phys. **193**, 206 (1989).
- [17] J. Hubbard, Proc. Royal Society **276**, 238 (1963).
- [18] A. J. Millis, R. Mueller, and B. I. Shraiman, Phys. Rev. B **54**, 5389 (1996).
- [19] S. Ciuchi and F. de Pasquale, Phys. Rev. B **59**, 5431 (1999).
- [20] J. P. Hague and N. d’Ambrumenil, J. Low Temp. Phys. **140**, 77 (2005).
- [21] W. Metzner and D. Vollhardt, Phys. Rev. Lett. **62**, 324 (1989).
- [22] A. Georges, G. Kotliar, and Q. Si, Int. J. Mod. Phys. B **6**, 705 (1992).
- [23] A. Georges, G. Kotliar, W. Krauth, and M. Rozenburg, Rev. Mod. Phys. **68**, 13 (1996).
- [24] M. H. Hettler, M. Mukherjee, M. Jarrell, and H. R. Krishnamurthy, Phys. Rev. B **61**, 12739 (2000).
- [25] T. Pruschke, D. L. Cox, and M. Jarrell, Phys. Rev. B **47**, 3553 (1993).
- [26] W. F. Brinkman and T. M. Rice, Phys. Rev. B **2**, 4302 (1970).
- [27] J. P. Hague, J. Phys.: Condens. Matter **15**, 2535 (2003).
- [28] A. Georges and G. Kotliar, Phys. Rev. B **45**, 6479 (1992).
- [29] M. Jarrell, Phys. Rev. Lett. **69**, 168 (1992).
- [30] R. Lortz, Y. Wang, S. Abe, C. Meingast, Y. B. Paderno, V. Filippov, and A. Junod, Phys. Rev. B **72**, 024547 (2005).
- [31] J. P. Hague, P. E. Kornilovitch, A. S. Alexandrov, and J. H. Samson, Phys. Rev. B **73**, 054303 (2006).
- [32] J. P. Hague, Phys. Rev. B **73**, 060503 (2006).
- [33] J. P. Hague, J. Phys.: Condens. Matter **17**, 5663 (2005).
- [34] Migdal’s theorem it is not a theorem in the mathematical sense, so we prefer to call it Migdal’s analysis in this article.

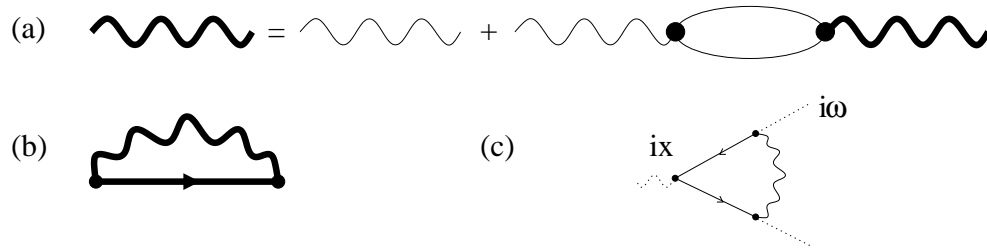


FIG. 1: (a) Dyson's equation for the phonon Green function to second order when vertex corrections are neglected. (b) Renormalized Fock diagram. (c) The first-order correction to the vertex function.  $ix$  is the frequency of the emitted phonon and  $i\omega$  is the frequency of the incoming electron. Neglect of this diagram is central to Migdal's theorem. Thick and thin lines represent the full and bare Green functions respectively. Wavy lines represent phonons and straight lines electrons.

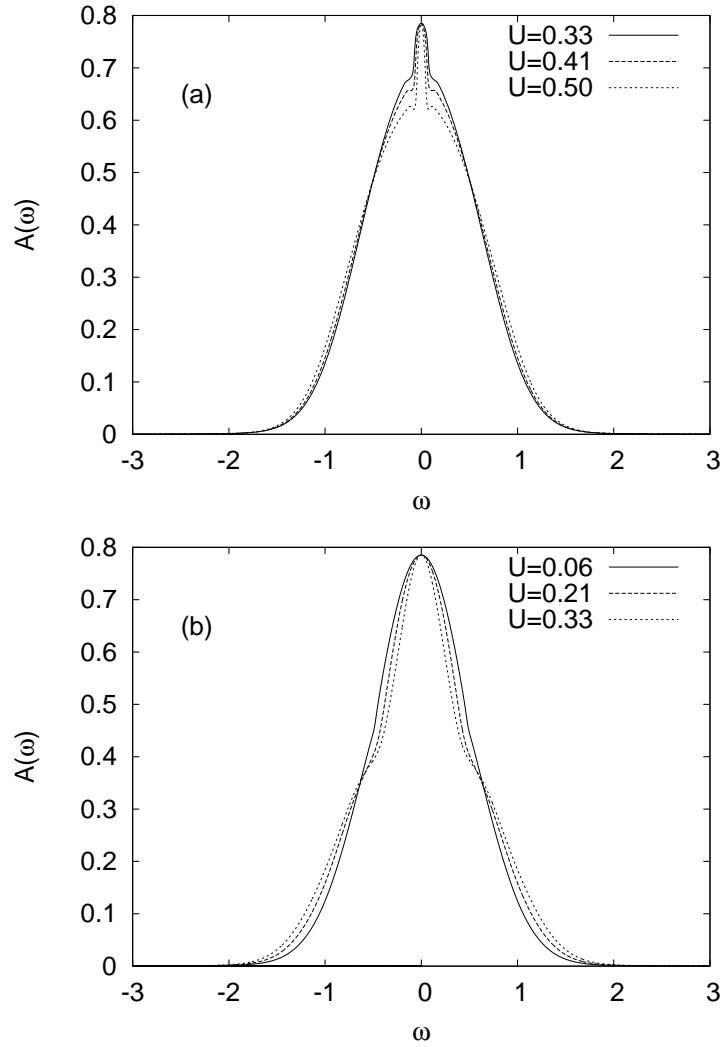


FIG. 2: Spectral functions of the Holstein model computed using Migdal-Eliashberg theory for  $\omega_0 = 0.125$  (panel a) and  $\omega_0 = 0.5$  (panel b) at  $T = 0$ . A bi-polaronic resonance forms at zero frequency. No upper and lower sub-bands are formed but spectral weight is shifted away from the Fermi-energy. The central peak narrows with increasing  $U$ , corresponding to a divergence in the effective mass. The general form of the curves is similar at all frequencies.

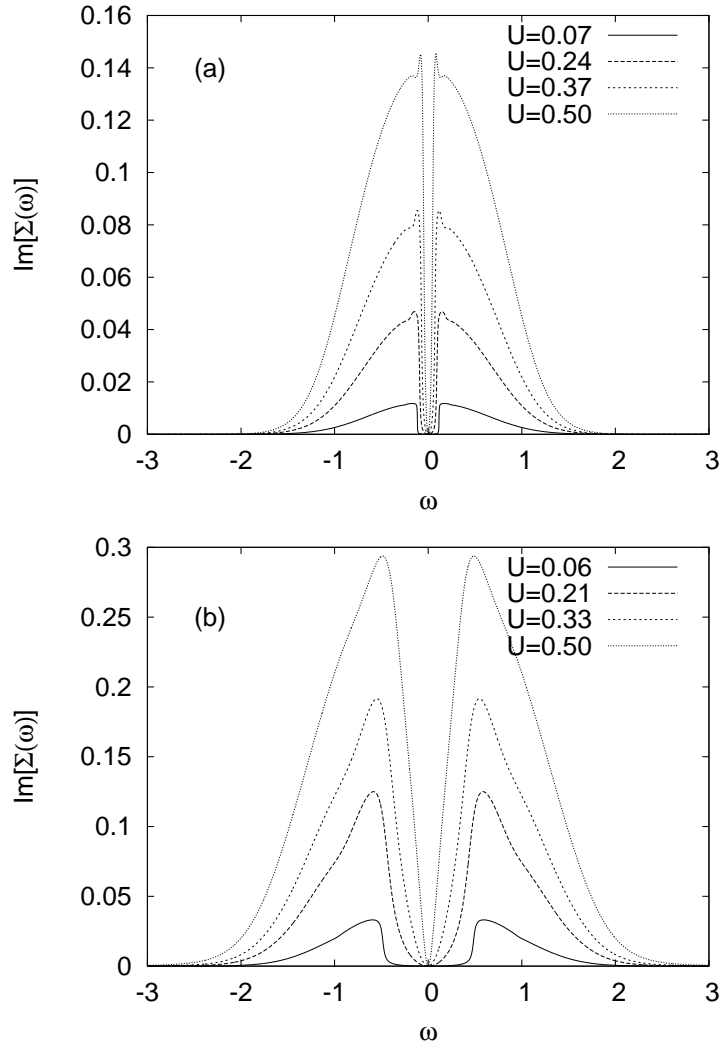


FIG. 3: Self-energy of the Holstein model solved using ME theory for  $\omega_0 = 0.125$  (panel a) and  $\omega_0 = 0.5$  (panel b) at  $T = 0$ . As the coupling,  $U = W\lambda$  (see discussion after eqn 2) increases, Hubbard-like behaviour is seen at low energy scales, and FK-like behaviour at  $|\omega| > \omega_0 = 0.2$ . Note how the gap in the self-energy at weak coupling (which is central to the Engelsberg–Schrieffer approach) fills up as coupling is increased. This is due to the increasing importance of higher order diagrams at stronger couplings. This shows that one should be careful about interpreting results from the cuprates ( $\lambda \gtrsim 1$ ) using an ES approach (this type of analysis is typically used on ARPES results), since the ES form for the self-energy (i.e. gapped at  $|\omega| < \omega_0$ ) can only be seen for very small  $\lambda$ .

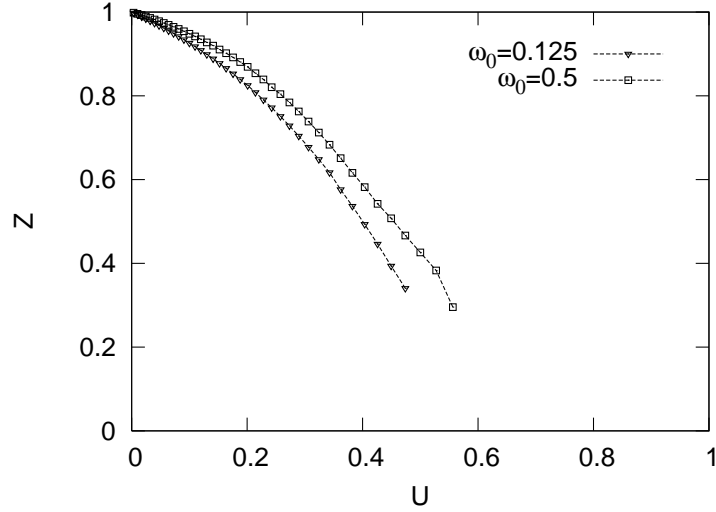


FIG. 4: Quasi-particle weight,  $Z$ , computed using ME theory as a function of  $U$  (results for phonon frequencies  $\omega_0 = 0.125$  and  $\omega_0 = 0.5$  are shown).  $Z$  is strongly renormalised for intermediate  $U$ .

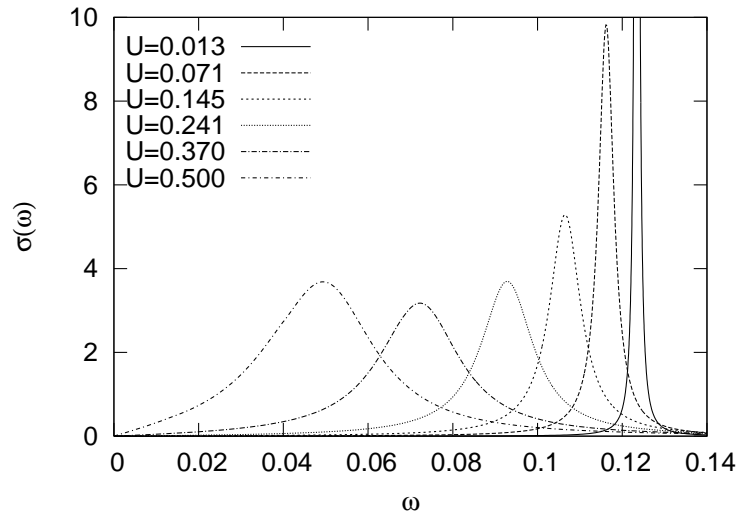


FIG. 5: Dependence of the phonon spectral function on coupling at  $\omega_0 = 0.125$ . The effective phonon frequency (location of maximum) and particle lifetime (inverse width of peak) are reduced with increasing coupling. When  $U = 0.5$  the curve is skewed in such a way that it is not Lorentzian, and the excitation no longer has the properties of a single phonon.



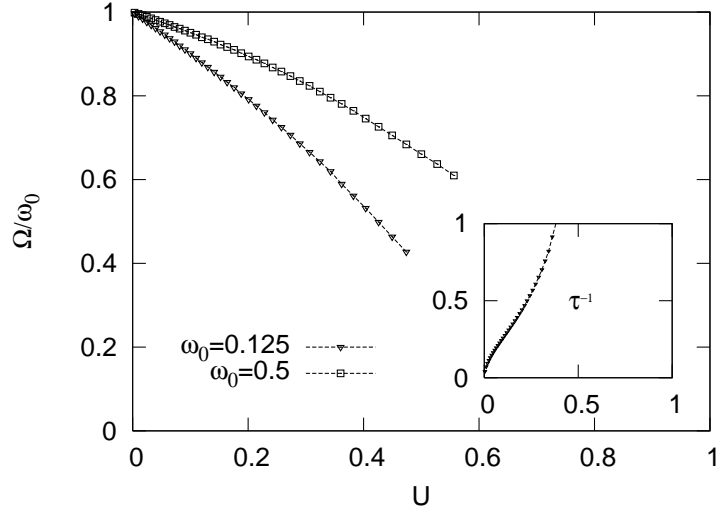


FIG. 6: Coupling dependence of the renormalised phonon frequency defined by  $\Omega^2 - \omega_0^2(1 + \text{Re}[\Pi_0(\Omega)]) = 0$ . The renormalisation of the effective phonon frequency is not as strong as that of the electronic inverse mass (quasi-particle weight  $Z$ ) shown in figure 4, which goes to zero at the transition. The inset shows the quasiparticle lifetime given by  $\sqrt{\text{Im}[\Pi_0(\Omega)]}$ . When the value of  $\lambda$  tends to 1, the phonons can no longer be treated as single particle excitations.

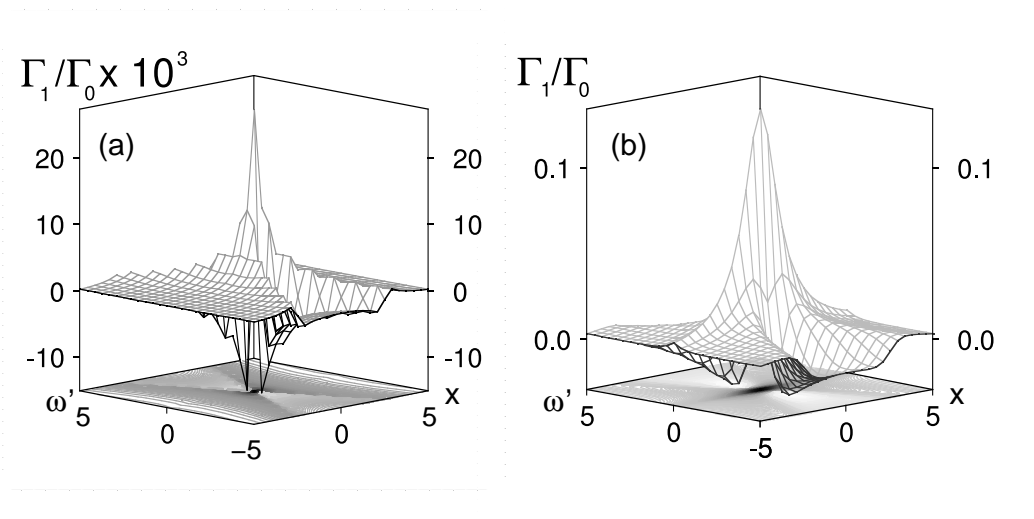


FIG. 7: The first order correction to the vertex function when (a)  $\omega_0 = 0.0556$  and  $U = 0.214$  (b)  $\omega_0 = 0.75$  and  $U = 0.214$ . The central maximum in (b) shows a ratio of over 10% and one should expect significant corrections to quantities computed within ME theory.

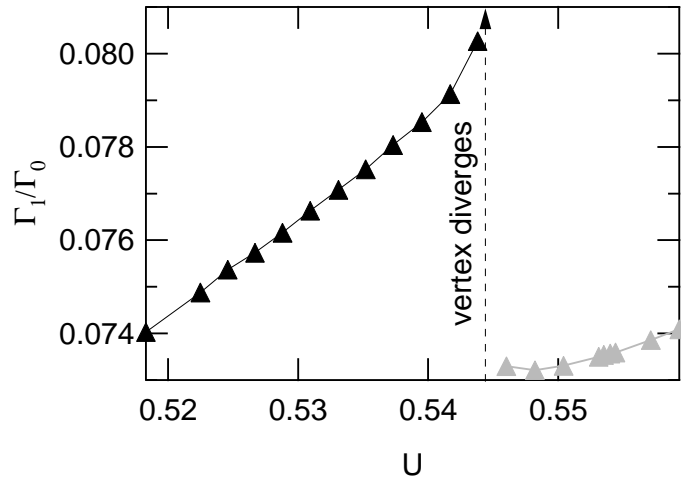


FIG. 8: Divergence in the vertex correction. At the divergence Migdal's analysis breaks down. Points for larger values of  $U$  (grey line) are shown in order to highlight the divergence but the ME treatment used here is not valid above the divergence, since the non-analyticity marks the limit of the expansion in  $\lambda$ .

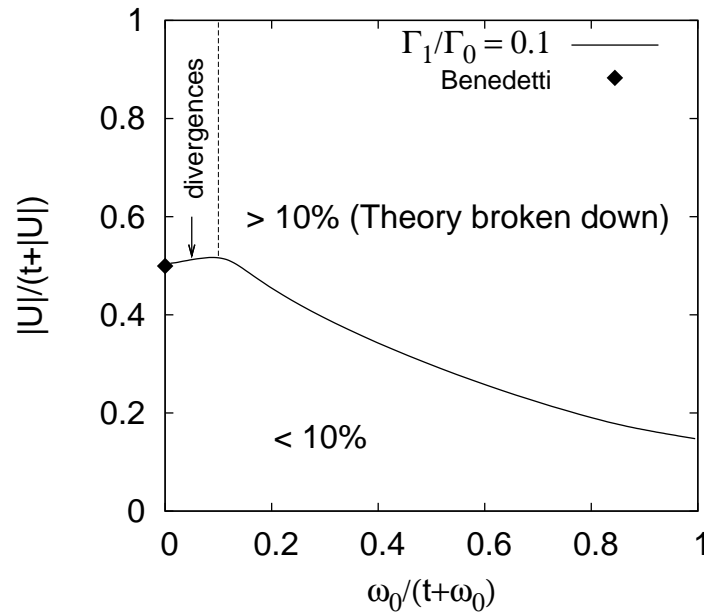


FIG. 9: Validity of ME theory as a function of  $U' = U/(U+t)$  and  $\omega'_0 = \omega_0/(\omega_0+t)$ , chosen so that a value of 1 represents  $U = \infty$ , etc. Also shown is the result of Benedetti and Zeyher for very low phonon frequency (filled diamond). Above the line, the ratio of the first order vertex correction to the bare vertex,  $\Gamma_1/\Gamma_0$ , exceeds 10% and ME theory is no longer strictly valid. At low frequencies (adiabatic limit), breakdown occurs at smaller coupling strength than expected as a result of the divergence found in the vertex corrections. This is in contrast to the interpretation of Migdal's analysis which is often used when low frequency experimental data is analysed, and is the main result of this article.

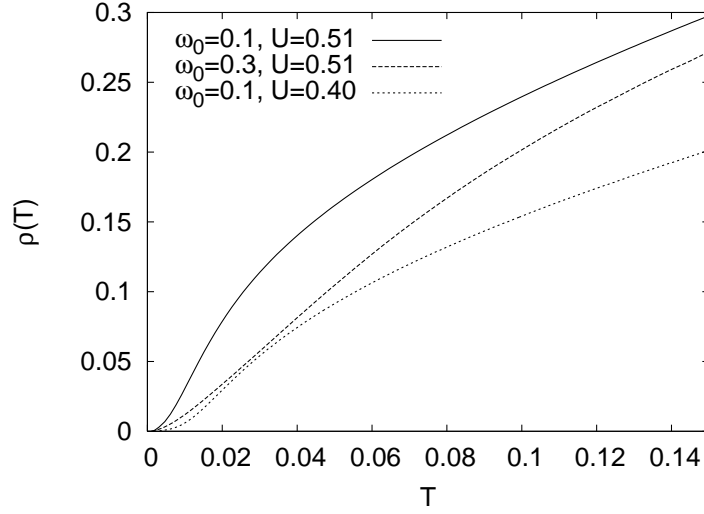


FIG. 10: Resistivity curves for various couplings and temperatures. The resistivity is in units of  $e^2V/ha^2$  with  $V$  the unit cell volume and  $a$  the lattice cell spacing. The temperature at which the shoulder appears is defined by the phonon frequency, and the amplitude is defined by the coupling. Low temperature behaviour is  $T^2$  according to a weakly renormalized electron gas. High temperature behaviour is linear. Note the negative curvature at intermediate temperature.